NASA Technical Memorandum 107030
AIAA-87-1814

Comparison of Fusion/Antiproton Propulsion Systems for Interplanetary Travel

Stanley K. Borowski
Lewis Research Center
Cleveland, Ohio

Prepared for the
23rd Joint Propulsion Conference
cosponsored by AIAA, ASME, SAE, and ASEE
San Diego, California, June 29—July 2, 1987

National Aeronautics and
Space Administration

Comparison of Fusion/Antiproton Propulsion Systems for Interplanetary Travel

Stanley K. Borowski*
National Aeronautics and Space Administration
Lewis Research Center
Cleveland, Ohio 44135

Abstract

Rocket propulsion driven by either thermonuclear fusion or antiproton annihilation reactions is an attractive concept because of the large amount of energy released from a small amount of fuel. Charged particles produced in both reactions can be manipulated electromagnetically making high thrust/high specific impulse (I_{sp}) operation possible. A comparison of the physics, engineering, and costs issues involved in using these advanced nuclear fuels is presented. Because of the unstable nature of the antiproton-proton ($\bar{p}p$) reaction products, annihilation energy must be converted to propulsive energy quickly. Antimatter thermal rockets based on solid and liquid fission core engine designs offer the potential for high thrust (~10^5 lbf)/high I_{sp} (up to ~2000 s) operation and 6 month round trip missions to Mars. The coupling of annihilation energy into a high-temperature gaseous or plasma working fluid appears more difficult, however, and requires the use of heavily shielded superconducting coils and space radiators for dissipating unused gamma ray power. By contrast, low-neutron-producing advanced fusion fuels (Cat-DD or DHe^3) produce mainly stable hydrogen and helium reaction products which thermalize quickly in the bulk plasma. The energetic plasma can be exhausted directly at high I_{sp} ($\simeq 10^5$s) or mixed with additional hydrogen for thrust augmentation. Magnetic fusion rockets with specific powers (α_p) in the range of 2.5 to 10 kW/kg and I_{sp} in the range of 20,000–50,000 s could enable round trip missions to Jupiter in less than a year. Inertial fusion rockets with $\alpha_p > 100$ kW/kg and $I_{sp} > 10^5$s could perform round trip missions to Pluto in less than 2 years. On the basis of preliminary fuel cost and mission analyses, fusion systems appear to outperform the antimatter engines for difficult interplanetary missions.

Introduction

capable of generating large amounts of jet power (P_{jet}). Because the thrust-to-engine weight ratio [F(kg)/M_W(kg) = 2000 α_p (kW/kg)/ g_o^2 I_{sp} (s)] of a spacecraft is directly proportional to the engine specific power ($\alpha_p \equiv P_{jet}/M_W$), large values of α_p are required to provide the acceleration levels necessary for rapid transportation of cargo and personnel throughout the solar system. An analysis of the yield from various energy sources (Table 1) indicates that only the nuclear fuels (fission, fusion, and synthetic antihydrogen fuels) can provide the power requirements for tomorrow's high-thrust/high-I_{sp} space drives.

For convenient interplanetary travel to become a reality, propulsion systems capable of operating in the middle to upper right portion of the P_{jet} vs I_{sp} plane (shown in Fig. 1) are required. Classical chemical (C) propulsion systems (occupying the left-hand side of Fig. 1) have a high-specific power capability [$\alpha_p \simeq 1550$ kW/kg for the Space Shuttle main engine (SSME)] but the power per unit mass of ejected matter is small (i.e., these systems operate at low I_{sp}) and great quantities of propellant are needed to essentially push propellant around. Electric propulsion (EP) systems use power from an onboard nuclear power source to accelerate propellant to high-exhaust velocities ($I_{sp} = 10^3$–10^4 s). However, the added weight of the power conversion and heat rejection systems and the efficiency toll of multiple energy conversion processes result in a low-specific power (~0.1 kW/kg) and restrict EP systems to low-thrust operation. Their high payload mass fraction capability can be exploited, however, for deep interplanetary or cargo transport missions.

Direct thrust nuclear propulsion systems (based on increasingly more sophisticated forms of nuclear energy conversion) provide the means of accessing the high-thrust/high-I_{sp} area of parameter space. Solid core fission thermal rockets (SCR) use the thermal energy released in the fission process to heat a working fluid (typically hydrogen), which is then exhausted to provide propulsive thrust. The SCR has a specific impulse [illegible] comparable to the electrothermal (ET) thruster (~10^3 s)

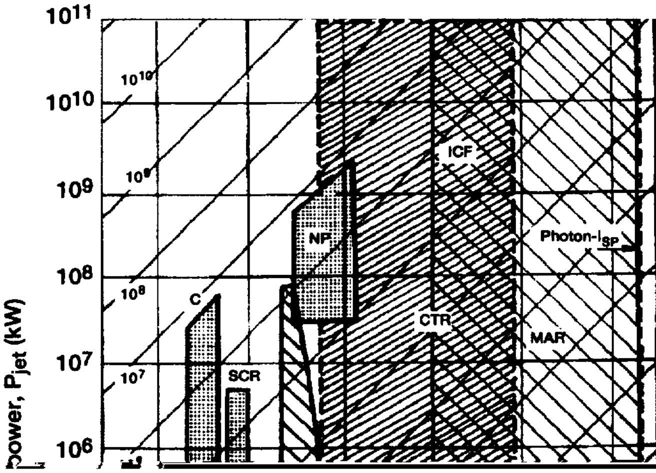

Nuclear propulsion is currently receiving greater attention by both NASA and the U.S. Air Force. In Refs. 3 and 4, the Air Force has identified the direct fission thermal rocket and the antiproton annihilation engine (MAR) as systems worthy of development. The interest in antimatter is attributed to the fact that it is a highly concentrated form of energy storage (see Table 1). A milligram of antihydrogen $\bar{\mathrm{H}}$ [consisting of an antiproton $\bar{p}$ and a positron e^+ (an antielectron)] reacted totally with the same amount of normal hydrogen possesses an energy content equivalent to ~ 13 t (1 metric ton (t) = 10^3 kg) of LO_2/LH_2. Although synthetic $\bar{\mathrm{H}}$ is definitely a "high-test" propellant, it requires a large energy investment and will be expensive to manufacture (~\$$10^{10}$/g assuming commercial electricity usage[5]), and difficult to store and manipulate. Estimates by Howe et al.[6] indicate that a production facility capable of

Table 1 Yield from various energy sources

Fuels	Reaction products	Energy release, J/kg	Converted mass fraction
		$(E/m_i = \alpha c^2)$	$\left(\alpha \equiv \frac{\Delta m}{m_i} = \frac{m_i - m_f}{m_i}\right)^a$
Chemical:			
Conventional: (LO_2/LH_2)	water, hydrogen,	1.35×10^{7}	1.5×10^{-10}
Exotics: atomic hydrogen,	common hydrogen,	2.18×10^{8}	2.4×10^{-9}
metastable helium	helium (He^4)	4.77×10^{8}	5.3×10^{-9}
Nuclear fission[b]:			
U^{233}, U^{235}, Pu^{239} (~200Mev/U^{235} fission)	radioactive fission fragments, neutrons, γ-Rays	8.2×10^{13}	9.1×10^{-4}
Nuclear fusion[c]:			
DT (0.4/0.6)	helium, neutrons	3.38×10^{14}	3.75×10^{-3}
Cat-DD(1.0)	hydrogen, helium, neutrons	3.45×10^{14}	3.84×10^{-3}
DHe^3 (0.4/0.6)	hydrogen, helium (some neutrons)	3.52×10^{14}	3.9×10^{-3}
pB^{11} (0.1/0.9)	helium (thermonuclear fission)	7.32×10^{13}	8.1×10^{-4}
Matter plus antimatter[d]:	Annihilation radiation		
$\bar{p}p$ (0.5/0.5)	pions, muons, electrons, positrons } Neutrinos and γ rays	9×10^{16}	1.0

[a]Δm is the change in mass between reactants (m_i) and products (m_f).
[b]U^{233}, U^{235}, Pu^{239} are fissile isotopes of uranium and plutonium.
[c]Weight composition corresponds to a 50/50 fusion fuel mixture; Cat-DD is the catalyzed DD reaction enhanced by burnup of reaction tritons (T) and helium-3 (He^3) nuclei with deuterons (D) in situ; B^{11} is the fusionable isotope of boron.
[d]Proton and Antiproton indicated by p, $\bar{p}$.

Considerations in the Use of Antiproton and Fusion Fuels

The energy content, reactivity, portability, availability, and practicality (in terms of charged particle output) are important considerations in the preliminary design of possible antiproton and fusion propulsion systems. A large energy yield per reaction or per kilogram of fuel is valuable only if it can be effectively used for propulsive thrust. Whereas antihydrogen fuel has a specific energy (E_{sp}) ~10^3 times that of fission and ~10^2 times that of fusion, this parameter can be misleading when viewed within the context of an actual propulsion system. For example, the fission process (*E*sp ~8.2x1013 J/kg) has a theoretical maximum specific impulse [Isp = $(2E\text{sp}/g_0^2)1/2$] of ~1.25x106s (assuming all of the fissionable mass is available for thrust generation). This is not the case in real reactor engine system, however, where the energy liberated in the fission process appears as heat in the reactor fuel rods. The core assembly is maintained at temperatures compatible with structural requirements by flowing liquid hydrogen through the reactor. In the NERVA nuclear rocket engine[8] hydrogen temperatures of ~2500 K at the nozzle entrance led to I_{sp} values of ~825 s. [Unlike the solid fission core reactors, in a magnetic fusion rocket engine the fusion fuel exits in a high-temperature plasma state and plasma power can be extracted using a magnetic diverter/nozzle configuration (discussed in Sec. III).] Whereas the I_{sp} of fission engines can be improved significantly by going to a gaseous fission core system[9], in the case of a solid core engine, technology limitations effectively reduce the specific energy of the fission fuel to ~3×10^7 J/kg - only a factor of ~2 better than LO_2/LH_2. In addition to the constraints imposed on engine design by the available technology, hardware requirements for storage, extraction and injection of hard-to-handle cryogenic and/or exotic fuel supplies can lead to excessive weight penalties (in terms of refrigeration mass, complex electromagnetic containers and transfer conduits, shielding, etc.) that may further degrade the perceived benefits of the fuel source.

Fusion Fuels

Table 2 shows the energy release and the reaction products associated with the various nuclear fuels. In the fission process a heavy uranium nucleus such as U^{235} is split into two fragments

Table 2 Released energy and products from various nuclear reactions

Typical fission :

$${}_{92}U^{235} + {}_0n^1 \rightarrow {}_{56}Ba^{137} + {}_{36}Kr^{97} + 2\,{}_0n^1 + \Delta E \ (\approx 200\ \text{MeV})$$

Fusion :

$${}_1D^2 + {}_1D^2 \xrightarrow{50\%} {}_1T^3 + {}_1p^1 + \Delta E \ (= 4.03\ \text{MeV}) \ \text{proton branch}$$

$$\xrightarrow{50\%} {}_2He^3 + {}_0n^1 + \Delta E \ (3.27\ \text{MeV}) \ \text{neutron branch}$$

$${}_1D^2 + {}_1T^3 \rightarrow {}_2He^4 + {}_0n^1 + \Delta E (= 17.6\ \text{MeV})$$

$${}_1D^2 + {}_2He^3 \rightarrow {}_2He^4 + {}_1p^1 + \Delta E (= 18.3\ \text{MeV})$$

$$6\,{}_1D^2 \rightarrow 2\,{}_2He^4 + 2\,{}_1p^1 + 2\,{}_0n^1 \ (\Delta E = 43.2\ \text{MeV}) \ \text{catalyzed--DD}$$

100% burnup of T and He^3 with D

$${}_1p^1 + {}_5B^{11} \rightarrow 3\,{}_2He^4 + \Delta E (= 8.7\ \text{MeV}) \ \text{thermonuclear fission}$$

$\bar{p}p$ Annihilation :

$$\bar{p} + p \rightarrow m\pi^0 + n\pi^+ + n\pi^- + \Delta E \ (\approx 1213\ \text{MeV}); m = n \approx 1.6$$

$$\pi^0 \xrightarrow{84\ \text{as}^a} 2\gamma \ (E_\gamma \approx 200\ \text{MeV})$$

$$\pi^+ \xrightarrow{70\ \text{ns}^b} \mu^+ + \nu_\mu \ (\text{muon neutrino})$$

$$\pi^- \xrightarrow{70\ \text{ns}} \mu^- + \bar{\nu}_\mu$$

$$\mu^- \xrightarrow{6.2\ \mu\text{s}^c} e^- + \nu_\mu + \bar{\nu}_e \ (\text{electron antineutrino})$$

$$\mu^+ \xrightarrow{6.2\ \mu\text{s}} e^+ + \nu_e + \bar{\nu}_\mu$$

$$e^- + e^+ \rightarrow 2\gamma \ (E_\gamma = 0.511\ \text{MeV})$$

[a]Attosecond = 10^{-18} s.
[b]Nanosecond = 10^{-9} s.
[c]Microsecond = 10^{-6} s.

with a release of considerable energy and the emission of neutrons and gamma rays. Energy can also be generated by fusing together light elements provided the temperature of the ionized mixture is sufficiently high (on the order of ~10^8–10^9 K) for the positively charged fuel ions to overcome their coulomb repulsion. The fuel cycles with the greatest reactivity at temperatures below 100 KeV (1 keV = 1.16×10^7 K) involve the hydrogen isotopes deuterium D and tritium T and the helium isotope He^3. The energy liberated in the fusion process is partitioned among the reaction products (which includes neutrons n, hydrogen p and helium He^4) and appears in the form of kinetic energy. The DT cycle has the largest reaction rate at low temperatures ($\leq$15 keV). Unfortunately it releases 80% of its energy in energetic (14.1 MeV) neutrons which can only be recovered in a complex tritium breeding blanket structure using thermal conversion equipment. Substantial quantities of shielding are also required for protection of crew and equipment (primarily the superconducting coils used to generate the plasma confining magnetic fields). The excessive weights involved in using DT appear to rule out its use for propulsion systems.

The DD fusion reaction is characterized by two branches (a neutron and a proton branch) which occur with roughly equal probability. By burning the tritium and He^3 resulting from these energy-poor reactions in the DD plasma itself, a catalyzed DD (Cat-DD) burn results, which has a significantly improved energy output (~14.4 MeV/pair of DD fuel ions burned). In addition, greater than 60% of the energy output from a Cat-DD reactor appears in the form of charged particles (protons and He^4). The attractiveness of the Cat-DD fuel cycle is that it is self-sufficient, i.e., it requires only naturally available deuterium as the main fuel feed. It is also relatively inexpensive (~\$$10^3$/kg) (Ref. 10) and abundant (estimates of the deuterium content in

source (~10^9 kg) of He^3 deposited on the lunar surface by solar wind bombardment.[11] It is estimated that this reserve could provide adequate He^3 for both propulsion and power production for many decades or until such time as the vast reserves (~10^{23} kg) of He^3 from Jupiter can be tapped.[11]

A final item of significance which could impact future DHe^3 usage deals with recent theoretical and experimental work[12,13] on the use of spin-polarized fusion fuels. Indications are that spin polarization of the DHe^3 nuclei (prior to reactor injection) can enhance the fuel's reactivity by 50% while simultaneously suppressing the troublesome neutron-producing DD side reactions. If the perceived benefits of spin polarized fuel are borne out in the future a clean, fusion-powered, manned planetary transportation system could be available in the first half of the 21st century. Finally, on a longer time scale the proton-based pB^{11} (boron-11 isotope) fuel cycle could lead to a superclean fusion engine which exhausts only helium-4 nuclei produced by a fusion reaction which is equivalent to thermonuclear fission.

Antiproton Annihilation

In contrast to the positron–electron (e^+e^-) reaction which emits two 0.511-MeV gamma rays, the antiproton–proton ($\bar{p}p$) reaction shown in Table 2 releases its considerable energy content (~1876 MeV/annihilation) primarily in the form of relativistic neutral and charged pions (or π mesons). Each pion possesses an average total energy [$E_t = E_0 + \Delta E = \gamma E_0$; $\gamma = 1 + (\Delta E/E_0)$] of ~390 MeV which consists of the particle's rest mass E_0 and kinetic energy ΔE components. The charged pions carry either a unit positive (π^+) or negative (π^-) electron charge and each has a rest mass energy of ~140 MeV. The neutral pion (π^0) has zero electric charge and is slightly lighter at ~135 MeV.

electrons and positrons can also annihilate yielding additional energy in the form of two 0.511-MeV gamma rays. The neutrinos are considered to be massless and move at essentially the speed of light. They are extremely penetrating and rarely interact with matter. Under vacuum conditions the various muon and electron neutrino particle–antiparticle pairs carry off ~50% of the available annihilation energy following a $\bar{p}p$ reaction.

The designer of antiproton propulsion systems, aware of this annihilation history, must device reactor/rocket engine configurations capable of 1) utilizing the tremendous energy content of the $\bar{p}p$ reaction products and 2) effectively accessing that range of exhaust velocities required for a particular mission. Because each π^0 meson decays almost immediately into two gamma rays, the particles which must be dealt with for thrust generation include 1) the high-energy charged pions (both the π^+ meson and its antiparticle, the π^- meson), 2) the generations of decay charged particles which follow (muons, electrons, and positrons), and 3) 200-MeV gamma rays. The charged particles can be either exhausted directly at high I_{sp} using a magnetic nozzle as discussed by Morgan,[15] or they can be trapped in a magnetic container and their kinetic energy used to heat a working propellant[15,16] for lower I_{sp} operation.

To put the energy in the charged pions to use for direct propulsive thrust, an axially diverging magnetic nozzle configuration can be employed to convert the perpendicular energy of the charged pions to directed energy along the nozzle axis. At a kinetic energy of 250 MeV, the directed pions will exit the nozzle at an exhaust velocity of $v_{ex} \simeq 0.94c$ (corresponding to a $I_{sp} \simeq 28.8\times10^6$ s). Assuming engine operation at the 100-lbf thrust level, the corresponding jet power is P_{jet} ($= Fv_{ex}/2$) $\simeq 62.7$ GW. Associating this power level with the charged pion exhaust (~2/3 of the total generated annihilation power), one finds that ~31.4 GW (~2.7×10^{10} Ci) of 200-MeV gamma-ray power is also being generated. Shielding sensitive spacecraft components (such as crew, ship electronics, and both cryogenic and superconducting coil systems for the magnetic nozzle) against this level of radiation and dissipating the heat appears impossible.

Depending on power level, the decay gamma energy can be recovered for propulsive purposes using a regeneratively cooled tungsten shield. Hydrogen flowing through channels in the shield and exiting at the nozzle throat could provide cooling for both components, as well as a source of hot hydrogen for thrust augmentation. However, the exclusive reliance on this open-cycle coolant mode deprives the antimatter rocket of one of its operational advantages, namely, the wide range of interchangeability of thrust and specific impulse. Operational flexibility can be maintained by employing a closed-cooling cycle space radiator system (discussed in Sec. III) capable of responding to thrust variations by varying the number of primary radiator modules in use. With such a system, an adequate cooling level is possible even during high I_{sp} operation when the hydrogen flow is reduced.

Specific impulse values more appropriate for interplanetary travel (~5000– 20,000 s) should be possible by allowing the charged pions to transfer their kinetic energy collisionally to a working gas. The resulting exhaust would have nearly the same energy content as the charged pion exhaust (assuming negligible losses for dissociation and ionization) but would generate increased levels of thrust due to the higher mass throughout. To achieve collisional coupling, the slowing down or stopping time of the charged pions in the working gas/plasma must be less than the pions mean life time. If the charged pions or muons decay before dissipating an appreciable percentage of their kinetic energy into the host gas/plasma, an increasing portion of the available annihilation energy will be lost in the form of unrecoverable neutrinos. This dissipation process is not trivial. As an example, we consider an antimatter rocket with a hydrogen working gas and a reaction chamber pressure and temperature of 200 atm (1 atm = 1.013×10^5 newtons) and 3000 K (corresponding to an I_{sp} ~1000 s). At these conditions the density ρ of H_2 is ~1.63×10^{-3} g/cm^3. The corresponding range of a 250-MeV charged pion is ~47.1 g/cm^2/$\rho \simeq 290$ m (Ref. 17) and the stopping time (~$\Delta\bar{E}_\pi/SP\cdot\rho\cdot\bar{v}$) is ~0.3 µs (~130 µs at 2000 atm). Here SP is the stopping power in MeV-cm^2/g (Ref. 17), and $\bar{v}$ is the average velocity of the charged pion. These values are orders of magnitude larger than the mean range and lifetime of the pion in vacuum. As a result, magnetic fields will be required to contain the energetic charged pions (and muons) within the reaction chamber, and superconducting magnets (requiring negligible recirculation power) will be a critical component of the annihilation engine design. Finally, because the average kinetic energy of a charged pion is roughly a factor of 20 larger than that of the most energetic fusion reaction product (a 14.7-MeV proton from the DHe^3 reaction), the pion gyroradius, given (in mks units) by

$$r_{gyro}(m) = \left(\gamma^2 - 1\right)^{1/2}\left[m_\pi c/eB(T)\right] \quad (1)$$

will be more than twice that of the proton for a given magnetic field strength B. [The parameters c and e are the speed of light and the electron charge (1.602×10^{-19} C), respectively.] To ensure adequate containment in antimatter rocket engines, magnetic field strengths higher than those currently being contemplated for use in fusion reactors will be needed.

Fusion and Antiproton Propulsion Concepts

Rocket propulsion driven by thermonuclear fusion or antiproton annihilation reactions is an attractive concept: a large amount of energy can be released from a relatively small amount of fuel, and the charged reaction products can be manipulated electromagnetically for thrust generation. Propulsion systems

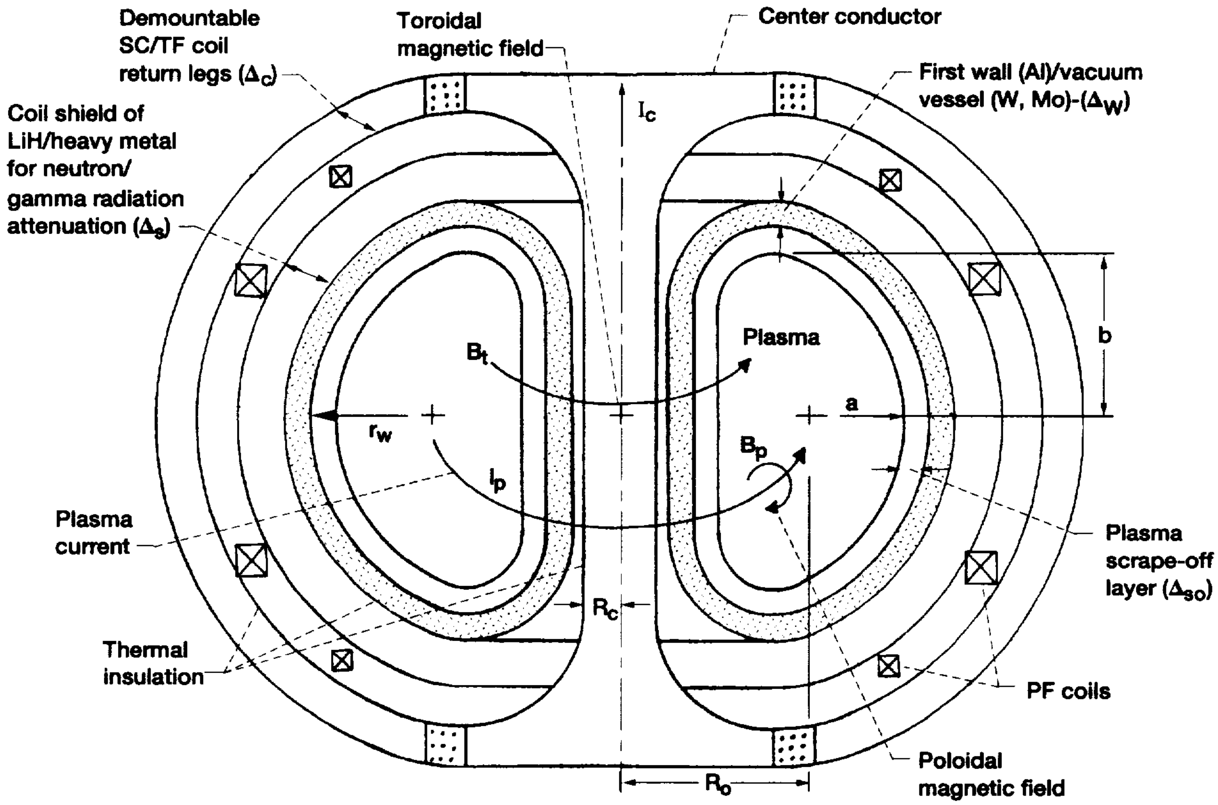

Figure 3.—Schematic of an advanced (spherical torus) tokamak reactor system.[21]

B_p can be comparable to B_t at the plasma outboard edge. Also, because of the large poloidal current component of I_p, plasma enhancement of the on-axis toroidal field (referred to as paramagnetism) is significant in the ST (a factor of ~2 larger than the vacuum field generated by the TF coils). Because of the ST's small aspect ratio, high-β operation is possible, however, standard inductive current startup techniques are difficult and efficient noninductive current drive techniques are required.[20] A cross section of the ST's magnetic field structure yields a set of nested poloidal magnetic field surfaces which exhibit toroidal symmetry. It is on these surfaces that the circulating hot-plasma particles are confined and across which they conduct heat and collisionally diffuse. By injecting supplementary heating (either as beams of energetic neutral atoms or as wave energy), the plasma temperature can be increased to the point where the plasma ignites, i.e., its reactivity is sufficiently high that the power of the charged fusion reaction products (P_{cp}) alone can maintain the fusioning plasma temperature against losses associated with radiation [both bremsstrahlung (P_{brems}) and synchroton (P_{synch})] and transport mechanisms. Exhausting this transport power P_{tr} for thrust generation and thermally converting the radiation loss (which can also include neutron radiation) for needed recirculation power are the key elements of a self-sustaining magnetic fusion rocket (see Fig. 4).

In terrestrial power reactor designs of the ST burning DT fuel only what is absolutely indispensable inboard of the plasma is retained. This includes a first wall/vacuum chamber arrangement and a normal center conductor that carries current to produce the tokamak's magnetic field. Other components, such as the solenoidal and inboard neutron shielding, are eliminated. The resulting devices have exceptionally small aspect ratios ($1.3 \sim A \sim 2.0$) and, in appearance look much like a sphere with a modest hole through the center, hence, the name spherical torus.

The potential for neutronless fusion power generation made possible through the use of spin-polarized DHe^3 has led to the examination of a high field ($B_t \sim 10$ T), superconducting version of the ST for rocket application.[21] The configuration is illustrated in Fig. 3 where we have speculated on the possibility of using demountable SC/TF coil legs to improve access to the internal torus and poloidal field coils. The central conductor is assumed to use a high field/high current density ($\lesssim 10^8$ A/m^2) superconductor employing an advanced vanadium–gallium alloy (V_3Ga) and an aluminum stabilizer for weight reduction.

For the spherical torus-based fusion rocket (STR) to operate continuously and at high-power output, it will be necessary to remove the nonfusionable thermalized charged particle ash (protons and He^4 ions) from the plasma. The magnetic bundle

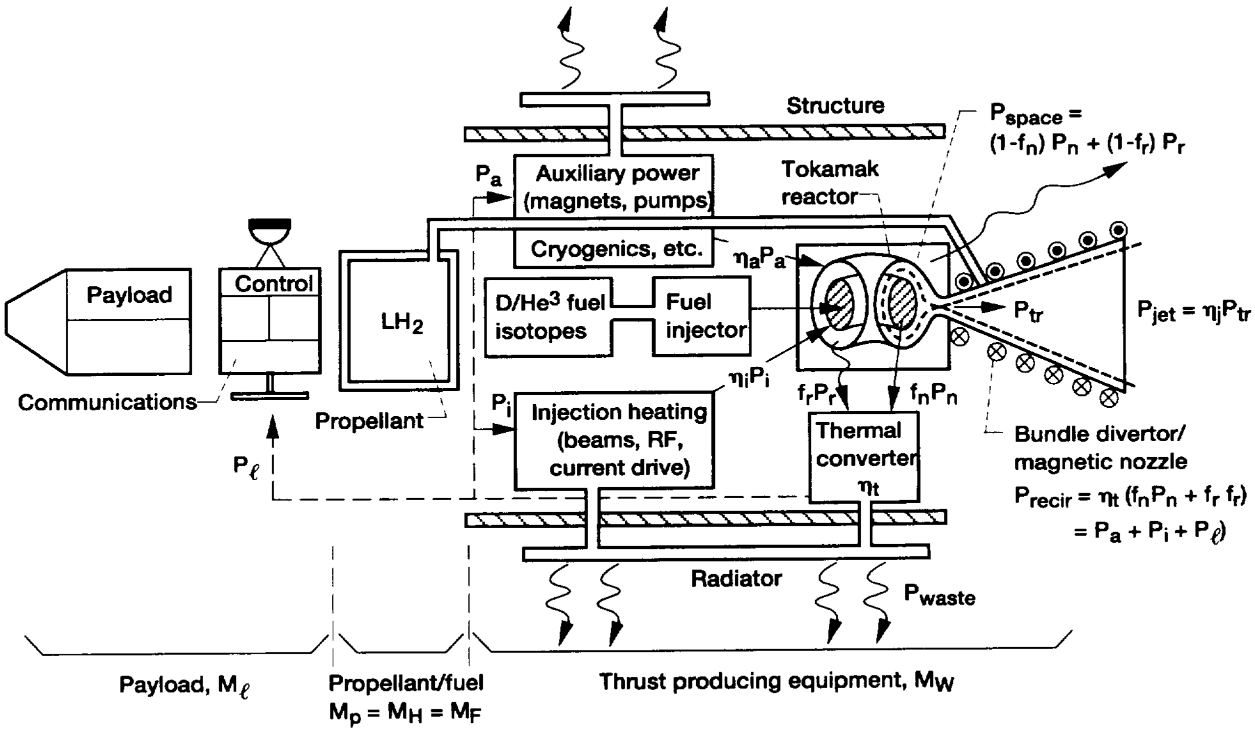

Figure 4.—Component and power flow diagram for an advanced tokamak fusion rocket.[21]

diverter[22] will be an important component for the STR, for it serves as a conduit for channeling plasma exhaust (including wall-generated impurities) out of the torus and into a magnetic field expander (nozzle) where the perpendicular plasma energy can be converted to directed energy along the nozzle axis.

The spheromak compact toroid (Fig. 5) is a low-aspect-ratio ($A \simeq 2$) plasma configuration which, like the tokamak, uses toroidal (B_t) and poloidal (B_p) magnetic fields for confinement. In the spheromak, however, the poloidally directed currents generating B_t flow in the plasma itself and not in external

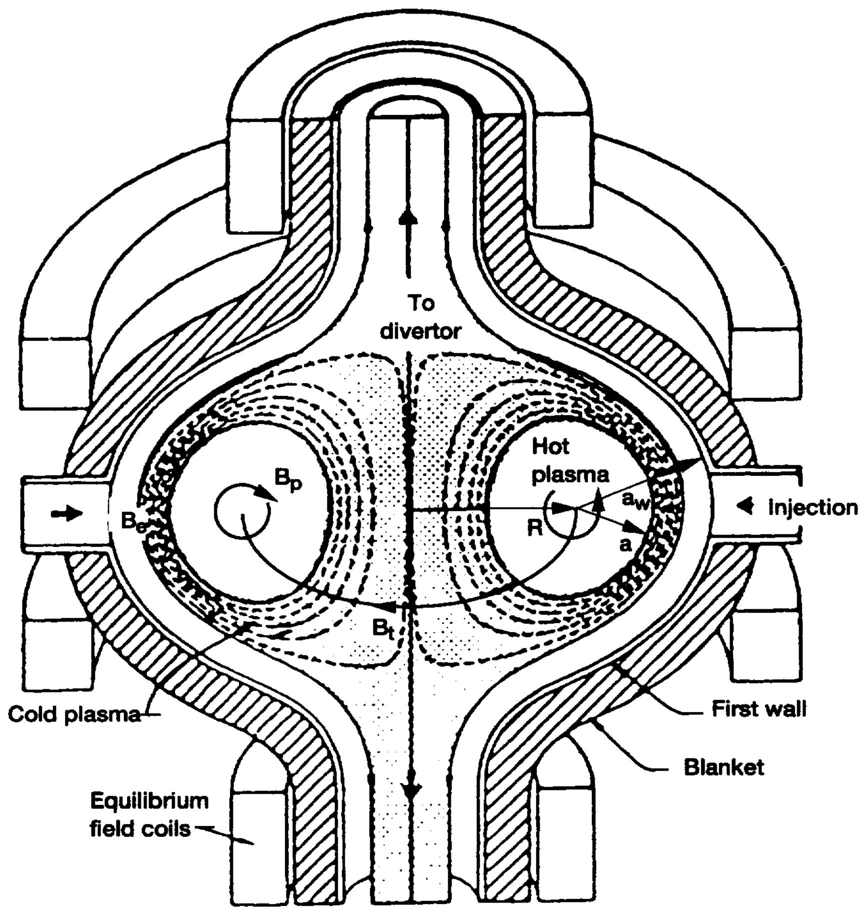

Figure 5.—High β potential and natural divertor action of the spheromak concept can be exploited for rocket thrust.[19]

Here $<n> = n_o/(1 + \delta_n)$, n_o and δ_n being the peak density on axis and density-profile shape factor, respectively, and $<\hat{T}> = T_o/[(1 + \delta_n + \delta_T)/(1 + \delta_n)]$, δ_T being the temperature profile shape factor. Rewriting Eq. (2) in the following form:

$$\beta_{eng} B_{coil}^2 = 5\mu_o k < nT >= 10^{-21} < n > \ < \hat{T} > \tag{5}$$

and specifying $<\hat{T}> = 50$ keV, one finds that $<n> \simeq 8\times10^{20}/\mathrm{m}^3$ (assuming flat profiles, i.e, $\delta_n = \delta_T = 0$) and $P_f/V_p \approx 25$ MW/m^3 for a 50/50 DHe^3 mixture [Eq. 3]. Spin polarization of the DHe^3 fuel can increase the power density by a factor of ~1.5, and density, and temperature profile peaking ($\delta_n = 1$, $\delta_T = 2$) by an additional factor of 2 yielding a final fusion power density of ~75 MW/m^3. Assuming the same power level used in the STR ($P_f = 7500$ MW), the spheromak with its higher power density requires a plasma volume ($V_p = 2\pi^2$ Aa^3) of only ~100 m^3 (as compared to ~227 m^3 for the STR). Preliminary calculations indicate that the overall spacecraft weight can be reduced by a factor of ~2.

The higher toroidal field [B_t (R_o) $\simeq$ 20 T] in the A = 2 spheromak case considered here leads to an increase in the synchrotron radiation power output ($\propto B_t^2$ nT) but a decrease in the bremsstrahlung output ($\propto n^2\ T^{1/2}$) because of the smaller plasma volume. With ~5500 MW available for jet power (assuming $P_{jet} = P_{tr}$), the specific power is estimated to be α_p ~10.5 kW/kg.

Lastly, the spheromak reactor will need very efficient current drive (about several amps per watt of sustaining current drive power) due to the large toroidal and poloidal currents in the device, ~70 and 270 MA, respectively. It is possible that preferential biasing of in situ synchrotron radiation[24] and the bootstrap effect caused by radial diffusion[25] can drive all or a substantial portion of the required currents in the spheromak during steady-state operation. Without an effective means to sustain the internal currents, the magnetic fields will decay providing resistive plasma heating on a magnetic diffusion time scale given by

$$\tau_{mag}(s) \simeq 10[a(m)]^2 [T(keV)]^{3/2} \tag{6}$$

fraction (~60%) of the Cat-DD fuel cycle] and ~710 MJ in the form of x-ray and neutron radiation. Additional propellant mass (~10 times that of the fuel loading) surrounds the pellet providing the ablative material and also augmenting the engine's propulsive thrust. The exhaust velocity (v_{ex}) and jet power are given by

$$v_{ex} = g_o I_{sp} = \eta_j \sqrt{2 E_{cp}/m_p} \tag{7}$$

and

$$P_{jet} = 1/2 m_p \nu v_{ex}^2 = \eta_j^2 \nu E_{cp} \tag{8}$$

where η_j is the efficiency of the magnetic nozzle in converting charged particle fusion energy E_{cp} to jet energy, m_p is the initial pellet mass (10 x m_c) and ν is pellet repetition rate. With ν = 100 Hz and η_j = 65%, the exhaust velocity and jet power are estimated to be ~2650 km/s (I_{sp} ~ 270 ks) and ~53 GW, respectively. The corresponding thrust level ($F = m_p \nu v_{ex}$) ~40 kN (~ 4 t). The

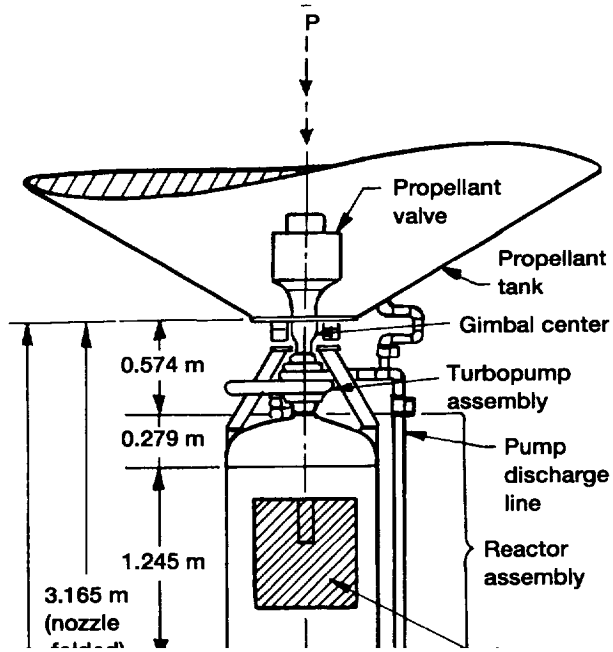

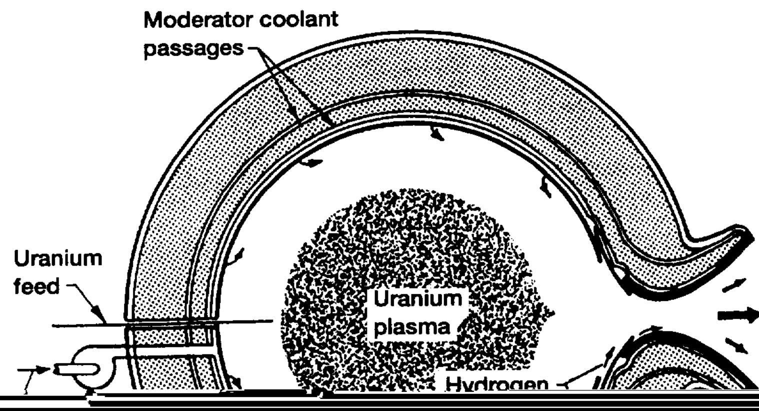
Moderator coolant passages
Uranium feed
Uranium plasma
Hydrogen

results are only ~3% smaller than those obtained using a maxwellian distribution, the simple estimates provided by Eq. (10) appear adequate.

To illustrate the characteristics of a possible magnetically assisted antimatter GCR, we assume its performance is comparable to that of a reference gas core fission rocket system[32] having the following parameters: P_{rx} = 1500 MW, P_{jet} = 1080 MW, $F = 4.4\times10^4$ N, I_{sp} = 5000 s, M_W = 70 t, $\alpha_p \simeq$ 15 kW/kg, D_c = 2.4 m, $\Delta_{mod} \simeq$ 0.8 m, $T_{rad} \simeq$ 1225 K and $V_f/V_c \simeq$ 25%. The parameters D_c, Δ_{mod}, T_{rad}, and V_f/V_c refer to the diameter of the reactor cavity, the moderator thickness, radiator temperature, and fuel-to-cavity volume ratio, respectively.

To estimate the field requirements for pion trapping we assume the tungsten plasma has the same approximate volume as the fission system. We also specify that $r_{gyro} \simeq 1/3R_f$ (to ensure adequate confinement of the annihilation debris within the tungsten). For a field strength in the magnetic well of $B_{min} \simeq$ 5 T and a mirror ratio of 3 (corresponding to $f_{T\pi} \simeq$ 82%), the mirror field $B_{max} \simeq$ 15 T. This field level requires the use of niobium-tin (Nb_3Sn) superconductor which has a maximum or critical current density of ~65 kA/cm^2 at ~15 T. And although the pion trapping fraction is high, there is still a substantial energy drain from the system attributed to neutrinos produced during decay of the unstable pions and muons.

Cassenti[16] has examined an antimatter-energized, magnetically assisted hydrogen thermal rocket for orbit transfer vehicle (OTV) applications. His analysis, which assumes 100% loss of gamma power, indicates that ~35% of the remaining annihilation energy can be transferred to the propellant. In the reference fission GCR 10% of P_{rx} reaches the solid, temperature-limited portions of the engine (moderator, etc.) whereas the remaining

shield/pressure vessel configuration the thickness of which can be determined using

$$I_\gamma(x)/I_\gamma(0) = \exp\left[-(\mu_e/\rho)\rho x\right] \qquad (12)$$

Here $I(x)/I(0)$ is the ratio of the gamma ray intensities [$I(0)$ being the intensity at the shield surface], μ_e/ρ is the material energy absorption coefficient [~0.1 cm^2/g for energetic gamma rays (E_γ > 100 MeV)] and ρx is the density (19.3 g/cm^3) times shield thickness which is proportional to the weight. For P_γ = 1350 MW and a tungsten thickness of 4 cm, the superconducting magnets see a heat load of ~0.6 MW$_t$. Because a modern liquid-helium refrigerator requires ~500 W$_e$ of electrical power to remove each watt of heat at 4.2 K and masses ~4 t/kW$_t$, such a heat load is intolerable for a portable propulsion system. At ~7 cm the heat load is down to ~2 kW$_t$ and can be handled by an 8 t refrigerator with ~ 1 MW of electrical power input.

For the antimatter GCR to operate at the same I_{sp}, propellant flow rate, and hydrogen inlet temperature as its fission counterpart (i.e., 5000 s, 0.9 kg/s and 1400 K) the external radiator must dissipate ~1332 MW of gamma power because only 18 MW can be removed regeneratively by the hydrogen propellant. Assuming a radiator specific mass of ~19 kg/m^2 and operating temperature of ~1225 K, the radiator mass is estimated to be ~193 t [M_{rad} (kg) $\simeq$ 145 Q_{rad} (MW) (Ref. 32)]. Increasing the radiator temperature to ~1500 K could reduce this value to 87 t.

Rather than dissipating the gamma power to space, it can be recovered by operating the tungsten at elevated temperatures (~3250 K) and introducing the hydrogen propellant into the reactor cavity at this value. Assuming the same level of jet

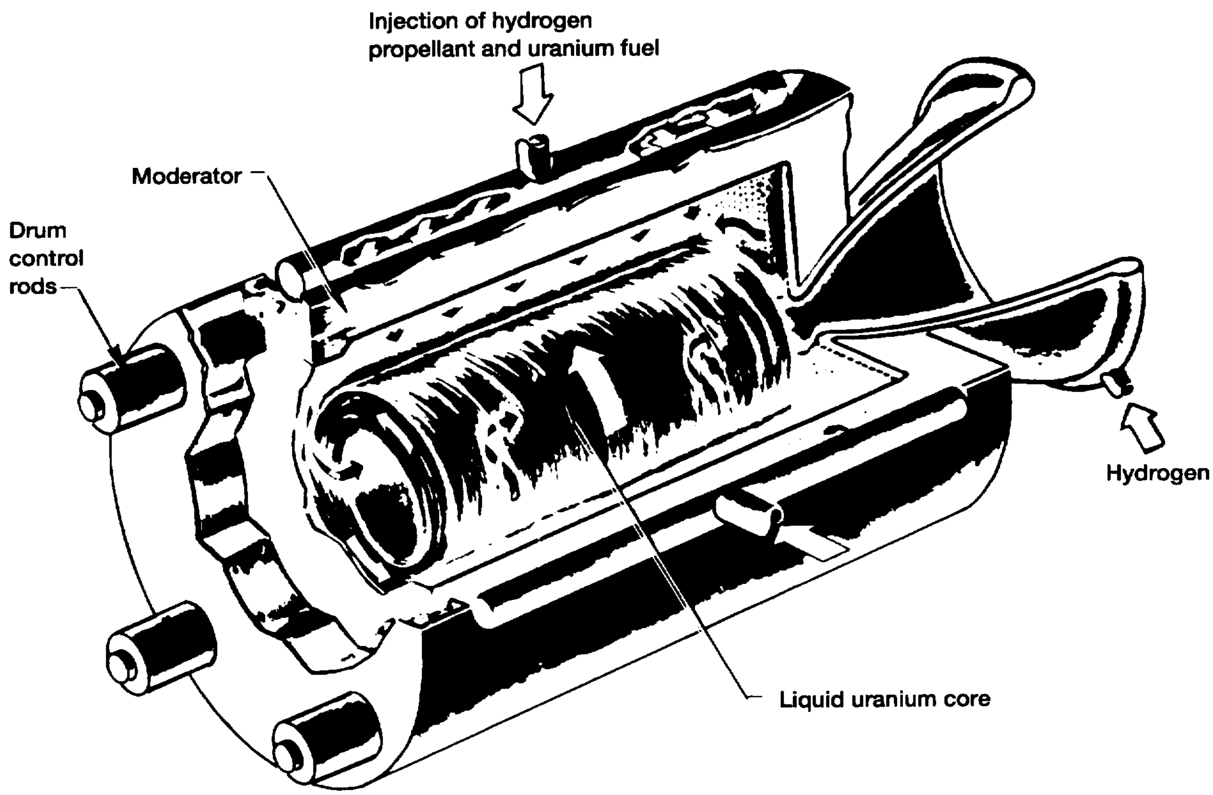

Figure 11.—Schematic of a liquid core fission rocket engine.

corresponding I_{sp} for the fission LCR is ~1300–1500 s for the same conditions. Over this I_{sp} range the F/M_W ratio is estimated to be ~2–10.[35] The limits on the fission LCR are attributed to increased vaporization of the nuclear fuel with increasing temperature and its subsequent entrainment in the hydrogen propellant which decreases the effective I_{sp}. One can assume similar difficulties with the antimatter LCR as the boiling-point temperature of tungsten is approached. However, with a F/M_W ~2 and an I_{sp} of ~2000 s, the specific power is quite attractive at ~190 kW/kg vs ~145 kW/kg for the fission LCR with the same

our application the magnet dimension is ~1/2 that of MFTF (at 1.5 m) but $B_{max} \simeq 15$ T. Using an aluminum stabilizer (~2.7 t/m^3) and vanadium-gallium (V_3Ga) superconductor (~6.1 t/m^3) with a 70% packing fraction (the remaining 30% of the coil cross sectional area containing coolant and structure), the coil weight is estimated to be ~70 t. Together with the radiator mass (estimated at 87 t for $T_{rad} = 1500$ K), the total engine weight is ~182 t. This results in a F/M_W ratio of ~2.5×10^{-2} and a specific power of ~5.9 kW/kg, a factor of 2.5 lower than that of the fission GCR.

simplicity that the specific impulse of a hydrogen plasma rocket is given by

$$I_{sp}(s) = \frac{1}{g_o}\sqrt{\frac{3kT_H}{m_H}} \simeq 1.73\times10^3\left[T_H(\text{eV})\right]^{1/2} \tag{13}$$

then I_{sp} in the range of 5,000–15,000 s should be possible with plasma exhaust temperatures of ~10–50 eV (1 eV = 1.16×10^4 K). From Eq. (2) the maximum plasma density that can be confined will depend on the available magnetic field strength and the β capability of the particular confinement concept. Assuming β = 50% and B = 15 T, the achievable densities are

$$n_e(\text{cm}^{-3}) \simeq \begin{cases} 1.5\times10^{19} & \text{for } T_e = 10 \text{ eV} \\ 3.0\times10^{18} & \text{for } T_e = 50 \text{ eV} \end{cases}$$

The ability to sustain the preceding plasma characteristics using an antiproton heating source can be determined using a simple plasma power balance

$$2/3\,P_{MA}/V_p = \left\{P_{\text{ion}} + P_{cx} + P_{\text{rad}} + P_{\text{tr}}\right\}/V_p \tag{14}$$

which neglects the gamma power component. The sink terms on the right refer to losses due to ionization of cold hydrogen gas, charge exchange of cold neutrals with warm ions, various radiation mechanisms and collisional diffusion processes.

At sufficiently high-ionization levels (which exist for $T_e \geq$ 10 eV) the neutral hydrogen density is low and ionization and charge exchange losses can be neglected to first order. Impurity radiation losses can also be ignored if one assumes a pure hydrogen plasma. Under these conditions bremsstrahlung radiation will be the primary nondiffusive energy loss mechanism. Bremsstrahlung (or braking) radiation is emitted when rapidly moving charged particles–mainly electrons—undergo a sudden deflection as a result of a near collision with a plasma ion. For a pure hydrogen plasma the bremmstrahlung power loss per unit volume is given by[38]

$$\frac{P_{\text{brems}}}{V_p}\left(\frac{\text{MW}}{\text{m}^3}\right) = 5.35\times10^{-43}\left[n_e(\text{m}^{-3})\right]^2\left[T_e(\text{keV})\right]^{1/2} \tag{15}$$

the plasma to reabsorb the emitted photons. The approximate mean free path for a bremsstrahlung photon in a hydrogen plasma is given by[39]

$$\lambda(\text{cm}) \simeq 10^{48}\left[T_e(\text{keV})\right]^{3.5}\Big/\left[n_e(\text{cm}^{-3})\right]^2 \tag{16}$$

Equation (16) assumes that the photon frequency ν is given by $h\nu = kT_e$ where h is Planck's constant (= 6.626×10^{-34} J/s). At T_e = 10 eV and $n_e = 1.5\times10^{19}$ cm^{-3}, $\lambda \simeq 4.5$ m. This distance increase to ~30 km for T_e = 50 eV and $n_e \simeq 3\times10^{18}$ cm^{-3}. It is only at very low temperatures ($\lesssim$5 eV) that adequate reabsorption occurs (e.g., $\lambda \simeq 2$ cm for $T_e \simeq 2$ eV and $n_e \simeq 1.5\times10^{19}$ cm^{-3}). The need to prevent excessive bremmstrahlung emissions through low-temperature operation leads to performance characteristics for the plasma rocket which are roughly equivalent to those found in the gas and liquid core versions of the antimatter rocket described earlier.

Even assuming that adequate reabsorption can occur at higher temperatures it is difficult for relativistic charged particles to slow down via plasma collisional effects. Consider a relativistic test particle with velocity V_T slowing down in a maxwellian plasma consisting of electrons and ions having thermal velocities V_{Te} and V_{Ti}. In the limiting case of $V_T > V_{Te} >> V_{Ti}$, the slowing down time is given (in cgs units with T in eV) by[40]

$$\tau_s(s) \simeq \frac{m_T^2 V_T^3}{4\pi n_e e^2 q_T^2 (2 + m_T / m_e)\ln\Lambda} \tag{17}$$

where m_T and m_e are the masses of the test particle and electron, respectively, q_T is the charge of the test particle, and $\ln\Lambda$ is the coulomb logarithm. For relativistic particles slowing is mainly due to scattering off of electrons. The slowing down time is also longer for heavier test particles implying that a charged pion ($m_\pi \simeq 273.5m_e$) will take longer to slow down than a muon ($m_\mu \simeq 206.5m_e$). For an average pion kinetic energy of 250 MeV, $V_T = V_\pi = c(\gamma^2 - 1)^{1/2}/\gamma \simeq 93.3\%c$, $q_T^2 = e^2$, $m_T \simeq 2.492\times10^{-25}$g and $\ln\Lambda \leq 5$ (assuming $n_e \simeq 1.5\times10^{19}$ cm^{-3} and $T_e \simeq 10$ eV), resulting in an average slowing down time of ~100 µs (almost 1500 times longer than the pion's relativistic lifetime of ~70 ns). Under such conditions the pions would decay into muons coupling little of their energy into the plasma. The muons, in turn, For fusion plasmas with $V_{Ti} < V_T < V_{Te}$, τ_s is given by[40]

$$\tau_s(s) = m_T^2 \Bigg/ \left\{ 4\pi n_e e^2 q_T^2 \left[\frac{Z}{V_T^3}\left(1+\frac{m_T}{m_i}\right) + \frac{4}{3\sqrt{\pi}}\left(1+\frac{m_T}{m_e}\right)\left(\frac{m_e}{2kT_e}\right)^{3/2} \right] \ln \Lambda \right\} \tag{18}$$

Both the electrons and ions contribute to slowing in a fusion plasma and a colder plasma can slow the test particles more quickly. For example, a 14.7 MeV proton ($Z = 1$) produced in a DHe^3 plasma operating at $n_e \simeq 7.5\times10^{14}$ cm^{-3}, $T_e \simeq 50$ keV, and $\ln \Lambda \simeq 17.5$ would slow down in ~525 ms. This is less than the characteristic energy confinement time of approximately several seconds which exists for most magnetic fusion reactors.

The preceding results indicate that stable fusion products are more effective in coupling their reaction energy into the bulk plasma than are the unstable pions and muons. Because of the poor coupling in an antimatter plasma rocket ~50% of annihilation energy could be lost in neutrinos. The 33% of the annihilation energy that appears as gamma power must be either dissipated via a heat rejection system (at the cost of additional spacecraft weight) or recovered regeneratively.

Some recovery seems prudent from an economics standpoint since an 18% conversion factor will require a factor of 5 increase in the amount of antihydrogen required for a given operating power level.

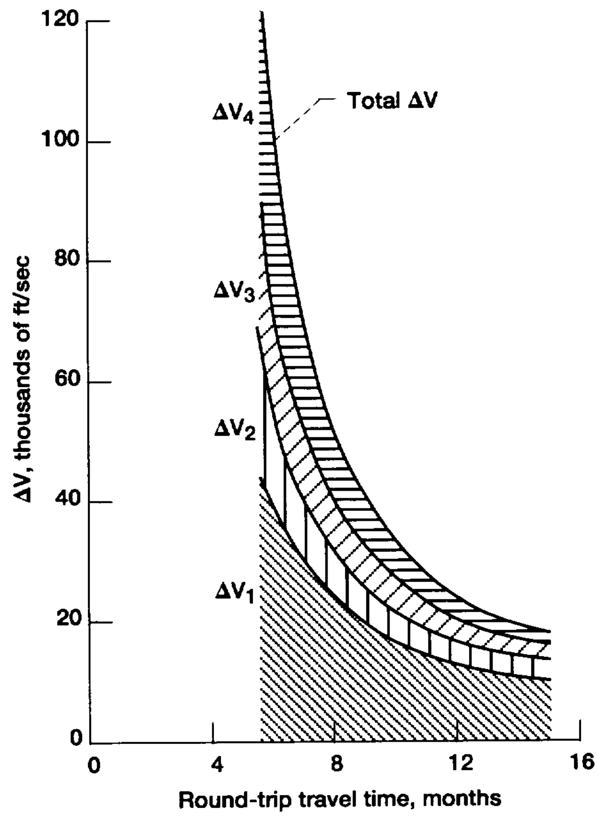

Figure 12.—Total velocity impulse required for round trip ballistic travel to Mar.[41]

Mission Performance Characteristics

Traditionally propulsion systems have been characterized as either high-thrust/ specific impulse-limited systems (such as chemical and nuclear fission rockets) or low-thrust/power-limited-systems (such as fission electric rockets). The antimatter systems we have discussed fit into the first category having flight profiles characterized by short burning periods separated by long coast periods. The fusion systems, however, provide a unique third category of engine capable of high thrust/high I_{sp} operation and fast interplanetary travel.

Antimatter Systems

In assessing the performance potential of the antimatter systems we have selected round-trip travel to Mars as the candidate mission. Simple estimates of the total velocity impulse (ΔV) for such a mission has been provided by Irving and Blum[41] as a function of the round-trip travel time in months (see Fig. 12). The four separate velocity increments, ΔV_1, ΔV_2, ΔV_3, ΔV_4, are those required for Earth escape, Mars capture, Mars escape, and Earth capture, respectively. By using the equations describing the system mass ratio ($R_M = M_i/M_f = \exp[\Delta V/g_0 I_{sp}]$; i and f denoting the initial and final mass of the spacecraft) and jet power ($P_{jet} = 1/2\ \dot{m}_p [g_o I_{sp}]^2$), the total engine burn time [t(s) $= M_p$ (kg)/ $\dot{m}_p$(kg/s)] can be expressed (in mks units) in the following form:

$$t_b = \frac{g_0^2}{2}\frac{I_{sp}^2}{P_{jet}}\left(M_W + M_L\right)\left(\exp\left[\Delta V/g_0 I_{sp}\right] - 1\right) \tag{19}$$

The parameter M_i ($= M_W + M_L + M_P = M_f + M_p$) is the initial spacecraft mass in Earth orbit and is composed of a propulsion system mass M_W, a payload mass M_L, and a propellant mass M_P. The dry mass of the spacecraft is denoted by M_f.

A 6 month quick trip ($\Delta V \simeq 30.5$ km/s) and a 1 year round-trip mission ($\Delta V \simeq 7.6$ km/s) to Mars have been selected as the candidate missions. Using Eq. (19) and its supporting equations, the system mass ratio, total engine burntime, and total propellant requirements have been estimated. The antiproton and uranium fuel inventories required for the mission have also been calculated along with an estimated fuel cost based on 5 M$/mg for antihydrogen[5] and ~ 50 k$/kg for enriched uranium. A summary of the performance characteristics for solid, liquid, and gaseous core antimatter systems, and their fission analogs, is found in Table 3. The solid and liquid core systems assume a thurst level of 10^5 lbf (~4.45×10^5N) and the GCR systems a value 1/10th of that at 10^4 lbf (~4.45×10^4N). The 6-month Mars mission is difficult for both the $\bar{p}$ and U^{235} versions of the NERVA engine. It requires large propellant loadings and substantial quantities of antihydrogen at significant cost. Payload delivery costs to low Earth orbit dominate total mission costs, however, and amount to ~$5.6 billion (5.6 B$) and ~10.4 B$ for the $\bar{p}$ and U^{235} systems, respectively, assuming a Saturn V-class launch vehicle with launch costs of ~$3300/kg (~$1500/lbm).

For the fission option the uranium fuel costs are low, requiring an investment of ~$12 million (M$) for the engine's critical fuel mass (M_{crit}) estimated at ~0.1 kg per megawatt of reactor power output ($P_{rx} = P_{jet}/\eta_j$).

The 582 mg of antihydrogen required for the Mars quick trip by the $\bar{p}$ NERVA concept can be reduced by optimizing the system specific impulse for minimum antihydrogen usage.[42] Minimum use is achieved when $I_{sp} = 0.63\,\Delta V/g_o \cong 1960$ s. The antimatter LCR concept operates near optimum conditions and could potentially perform the 6-month Mars mission with an initial mass in Earth orbit (IMEO) of ~474 t. The fission version of the LCR limited to an I_{sp} of ~1500 s due to enhanced fuel vaporization has a higher IMEO (~795 t). The F/M_W was specified at ~3.2 for the LCR systems (half the value in the $\bar{p}$ NERVA system) because of the need for a thick external moderator/reflector necessary to ensure neutron economy in the fission system. The radiator-cooled gas core fission rocket

Table 3 Summary of antimatter and fission engine performance

ΔV, km/s	R_M	t_b, h	M_p, t	$M_{\bar{p},u}$, mg/kg	Launch/Fuel costs
$\bar{p}$ NERVA: $P_{jet} = 2386$ MW, $I_{sp} = 1100$ s, $\dot{m}_p = 41$ kg/s, $\dot{m}_{\bar{p}}$ 15 μg/s, $M_W + M_L = 100$ t					
30.5	16.9	10.8	1590	582	5.6 B$/2.9 B$
7.6	2.02	0.69	102	37	0.7 B$/0.2 B$
NERVA: $P_{jet} = 1963$ MW, $I_{sp} = 900$ s, $\dot{m}_p = 50.4$ kg/s, $M_u = M_{crit}$ kg, $M_W + M_L = 100$ t					
30.5	31.7	16.9	3066	222	10.4 B/$ 11.7 M$
7.6	2.37	0.76	137.9	222	0.8 B$/11.7 M$
$\bar{p}$ LCR: $P_{jet} = 4362$ MW, $I_{sp} = 2000$ s, $\dot{m}_p = 22.7$ kg/s, $\dot{m}_{\bar{p}} = 26.1$ μg/s, $M_W + M_L = 100$ t					
30.5	4.74	4.58	374	430	1.6 B$/2.2 B$
7.6	1.47	0.58	47.4	54.5	0.5 B$/0.3 B$
Fission LCR: $P_{jet} = 3267$ MW, $I_{sp} = 1500$ s, $\dot{m}_p = 30.2$ kg/s, $M_u = 4\,M_{crit}$ kg, $M_W + M_L = 100$ t					
30.5	7.95	6.39	695	1400	2.6 B$/70 M$
7.6	1.68	0.63	68.5	1400	0.6 B$/70 M$
$\bar{p}$ GCR: $P_{jet} = 1080$ MW, $I_{sp} = 5000$ s, $\dot{m}_p = 0.9$ kg/s, $\dot{m}_{\bar{p}} = 22.5$ μg/s, $M_W + M_L = 282$ t					
30.5	1.86	75.0	243	6075	1.7 B$/30.4 B$
7.6	1.17	14.8	48.0	1199	1.1 B$/6.0 B$
Fission GCR: $P_{jet} = 1080$ MW, $I_{sp} = 5000$ s, $\dot{m}_p = 0.9$ kg/s, $M_u = \dot{m}_u t_b + 100$ kg, $M_W + M_L = 170$ t					
30.5	1.86	45.2	146	830	1.0 B$/41.5 M$
7.6	1.17	8.94	29.0	245	0.7 B$/12.3 M$

offers the best performance of all the $\bar{p}$ and fission systems examined. Because the GCR engine featured here is an open cycle design,[32] a quantity of U^{235} fuel ($\dot{m}_u/\dot{m}_p \sim 0.5\%$) is exhausted from the engine along with the hydrogen propellant. Added to this amount of lost U^{235} are four critical core loadings (each at ~25 kg) required for the four major propulsion maneuvers. The $\bar{p}$ GCR suffers from very high-fuel costs attributed to the larger engine weight (~182 t vs 70 t for fission GCR) and the poorer coupling of the annihilation products to the working fluid.

Fusion Systems

High-power fusion rockets possess the best attributes of both fission thermal engines (prolonged operation at relatively high thrust) and the fission-powered electric propulsion systems (high I_{sp}). It is envisioned that the fusion spacecraft would depart from and return to geosynchronous Earth orbit (GEO). In traveling between planetary bodies, the sun is considered to be the only source of gravitational force. Because the initial acceleration levels for the fusion systems examined here range from ~3–5×10^{-3} g_o (mg_o) (compared to the sun's gravitational pull of ~0.6 (mg_o) straight line trajectories can be assumed. To illustrate the performance potential for the fusion systems we have considered one-way and round-trip continuous burn acceleration/deceleration trajectory profiles which assume constant I_{sp}, F, and P_{jet} operation. The equations describing the transit times for the outbound and return legs of a journey from A to B (and back again) along with the distances traveled are given by[21]

$$\tau_{AB}(s) = \frac{I_{sp}(s)}{F/W_f}\left(\frac{1}{\beta}\right)\left(\frac{1}{\alpha}-1\right) \tag{20}$$

$$\tau_{BA}(s) = \frac{I_{sp}(s)}{F/W_f}\left(\frac{1}{\beta}-1\right) \tag{21}$$

$$\tau_{RT}(s) = \tau_{AB} + \tau_{BA} = \frac{I_{sp}(s)}{F/W_f}\left(\frac{1}{\alpha\beta}-1\right) \tag{22}$$

$$D_{AB}(m) = \frac{g_o\, I_{sp}^2(s)}{F/W_f}\left(\frac{1}{\beta}\right)\left(\frac{1}{\sqrt{\alpha}}-1\right)^2 = D_{BA} \tag{23}$$

$$D_{BA}(m) = \frac{g_o\, I_{sp}^2(s)}{F/W_f}\left(\frac{1}{\sqrt{\beta}}-1\right)^2 \tag{24}$$

where $W_f = M_f g_o$ is the dry weight, $1/\alpha = M_i/M_B$ ($M_B = M_f + M_p^{B\rightarrow A}$; $M_p^{B\rightarrow A}$ being the propellant used in traveling from B to A), $1/\beta \equiv M_B/M_f$, and $R_M = 1/(\alpha\beta)$. By specifying a particular planetary mission and its distance from Earth (1 astronomical unit (AU) = 1.495×10^{11} m), Eqs. (23) and (24) can be used to determine $1/\alpha$ and $1/\beta$ and their product, the spacecraft mass ratio. By knowing the mass of the thrust producing system (M_W) and specifying a payload mass (M_L) the IMEO, propellant requirements, and trip times can be calculated. Assuming a planetary refueling capability, Eqs. (21) and (24) can also be used to calculate one-way results. In this case $R_M = 1/\beta$.

The performance characteristics for a spherical torus, spheromak and inertial fusion rocket are summarized in Tables 4–6. Table 4 indicates that with planetary refueling possible, the STR can journey to Mars in ~34 days. The IMEO

Table 4 Spherical torus fusion rocket performance
STR characteristics

Polarized DHe^3, I_{sp} = 20 ks, $\dot{m}_p$ = 0.308 kg/s, α_p = 5.75 kW/kg, M_W = 1033 t, M_L = 200 t

One-way continuous burn/constant I_{sp} trajectory profile:

Mission[a]	D_{AB}, AU	R_M	M_i, t	M_p, t	M_L/M_i, %	τ_{AB}, days	a_i, 10^{-3} g_o
Mars	0.524	1.732	2135	902	9.4	33.9	~2.9
Ceres	1.767	2.497	3079	1846	6.5	69.4	2.0
Jupiter	4.203	3.590	4427	3194	4.5	120.0	~1.4

Round-trip trajectory results:

Mission[a]	R_M (= $1/\alpha\beta$)	$M_p^{A\rightarrow B}$	$M_p^{B\rightarrow A}$	$M_p^{A\rightarrow A}$	M_i	τ_{AB}	τ_{BA}	τ_{RT}
Mars	2.664	1149	902	2051	3284	43.2	33.9	77.1
Ceres	4.667	2675	1846	4521	5754	100.5	69.4	169.9
Jupiter	7.783	5169	3194	8363	9596	194.3	120.0	314.3

[a]Closest approach distances to Earth.

Table 5 Spheromak fusion rocket performance
SFR characteristics

Polarized DHe^3, $I_{sp} = 50$ ks, $\dot{m}_p = 4.95\times10^{-2}$ kg/s, $\alpha_p \simeq 11.5$ kW/kg, $M_W = 515$ t, $M_L = 200$ t

Round-trip continuous burn/constant I_{sp} trajectory profile:

Mission[a]	D_{AB}, AU	R_M	M_i, t	M_p, t	M_L/M_i, %[b]	τ_{AB}, days	τ_{RT}, days
Mars	0.524	1.465	1047	332	19.1	40.6	77.6
		(1.222)	(872)	(157)	(23.0)	(36.7)	---
Ceres	1.767	1.923	1375	660	14.5	83.2	154.0
Jupiter	4.203	2.55	1823	1108	11.0	114.4	258.7

[a]Closest approach distance to Earth.
[b]For outbound leg of journey.

Table 6 Inertial Fusion Rocket Performance
IFR characteristics

Cat-DD, $I_{sp} = 270$ ks, $\dot{m}_p = 0.015$ kg/s, $\alpha_p = 110$ kW/kg, $M_W = 486$ t, $M_L = 200$ t

Round-trip continuous burn/constant I_{sp} trajectory profile:

Mission[a]	D_{AB}, AU	$R_M (= 1/\alpha\beta)$	M_i, t	$M_p^{A\to A}$, t	M_L/M_i, %[b]	τ_{AB}, days	τ_{RT}, days
Mars	0.524	1.104	757.3	71.3	26.4	27.7	55.0
Ceres	1.767	1.196	820.5	134.5	24.4	53.1	103.7
Jupiter	4.203	1.309	898	212.0	22.3	84.6	163.6
Saturn	8.539	1.453	997	311.0	20.1	125.5	239.8
Uranus	18.182	1.689	1159	473.0	17.3	194.1	364.7
Neptune	29.058	1.901	1304	618.0	15.3	257.3	476.9
Pluto	38.518	2.063	1415	729.0	14.1	306.6	562.7

[a]Closest approach distances to Earth.
[b]For outbound leg of journey.

is 2135 t of which ~42% is propellant, 9.4% is payload and 48% is engine. The initial acceleration level is ~3 mg_o which is 5 times the value of the sun's gravitational pull at Earth. Jupiter can also be reached in ~4 months with a propellant loading of ~3200 t. Without a planetary refueling capability, the spacecraft must carry along sufficient propellant for the return trip. This requirement increases the overall IMEO and mission duration. The spheromak being lighter can operate at reduced propellant flow rates and higher specific impulse and still maintain initial acceleration levels of several milligees. With the SFR round-trip missions to Jupiter of ~8.5 months are possible with an IMEO ~1823 t and with a payload mass fraction of over 10%. (In all of the results shown, it is assumed that an equivalent amount of payload is returned.) The SFR can also perform one-way missions to Mars in ~37 days with initial mass requirements under 875 t (results shown in parentheses).

The STR and SFR results assumed the use of spin polarized DHe^3 in order to eliminate neutron radiation and obtain a lighter spacecraft. If the benefits of spin polarized DHe^3 are not achievable, magnetic fusion engines can still burn deuterium but at the expense of increased mass. By exploiting the high repetition rate and target gain possibilities of inertial confinement fusion, the IFR can not only burn abundant deuterium fuel efficiently, but it can do so with a relatively lightweight engine system (<500 t) (see Table 6). And whereas MCF rockets can reach out into the solar system by employing planetary refueling, the IFR can perform round-trip missions to Pluto (carrying a 200 t payload) in ~18.5 months (no refueling required). The IMEO would be 1415 t with propellant and payload mass fractions of ~52% and ~14%, respectively. We know of no other advanced propulsion concept with this capability. Tritium would be bred onboard the spacecraft to facilitate ignition of the DD fuel pellets and the deuterium fuel load which comprises ~10% of the propellant inventory would cost ~73 M$ at current prices of ~$$10^3$/kg.

Conclusions

The purpose of this chapter has been to compare various antimatter and fusion rocket concepts in an effort to obtain a clearer understanding of the advantages and disadvantages associated with each system. The areas examined have included fuel cycle characteristics, physics and technology requirements, mission performance capability, and fuel cost and availability issues. A number of subject areas have not been addressed. These include the antiproton reactivity issue at elevated temperatures, methods for injecting antiprotons into high-pressure gas/plasma reaction chambers, the effect of pion–nucleon collisions on slowing down, and the assumption of lightweight systems for the storage, extraction, and injection of antiprotons. All of these issues are expected to be important in the realization of a working anitmatter system.

On the basis of preliminary results obtained thus far, antimatter thermal rockets utilizing solid and liquid fission core reactor concepts offer the potential for high-thrust (~4.5×10^5 N)/high I_{sp} (up to ~2000 s) operation. The antimatter liquid core engine is capable of 6-month round-trip missions to Mars with IMEO <500 t and a system mass ratio of ~4.75 close to the optimum value of 4.9 obtained for minimum antihydrogen usage. The fuel costs are still large, however, because of the substantial IMEO requirements for the Mars mission. Furthermore, the $\bar{p}$ LCR is outperformed by the radiator-cooled, fission GCR in terms of IMEO, launch and fuel costs which brings into question the rationale for developing the more complex $\bar{p}$ system.

The coupling of the annihilation energy contained in the relativistic charged particles appears more difficult in high-temperature gaseous or plasma working fluids. Because high-field (>10 T) superconducting coils will be needed to improve energy coupling, they must be heavily shielded to minimize the power and mass requirements of the refrigeration system. In addition to a substantial radiation shield and magnet mass, an antimatter gas core design would require a large space radiator to dissipate unwanted gamma-ray power. Regenerative cooling of the shield/pressure vessel configuration requires a significant propellant flow rate into the cavity due to the large gamma power component. This quickly overwhelms the high I_{sp} feature of the gaseous core concept.

By contrast, fusion rocket engines burning the advanced fusion fuels Cat-DD or DHe^3 produce mainly stable hydrogen and helium reaction products which quickly thermalize in the bulk plasma. The bremsstrahlung power loss, which is emitted primarily in the soft x-ray photon range, can also be readily handled in a lightweight shield/blanket configuration and used to generate recirculating power for the system. The energetic particles which collisionally diffuse out of the plasma can be exhausted directly at high I_{sp} (<10^5 s) or mixed with additional hydrogen for thrust augmentation. Magnetic fusion engines with specific powers in the range of 2.5–10 kW/kg and I_{sp} of 20,000–50,000 s could enable round-trip missions to Jupiter in less than a year. Inertial fusion rockets with α_p >100 kW/kg and I_{sp} > 10^5 s offer outstandingly good performance over a wide range of interplanetary destinations and round-trip times. Even Pluto is accessible with round-trip travel times of less than 2 years. Finally, whereas synthetic antihydrogen must be manufactured, stable fusion fuels are found in abundance throughout the solar system (particularly the outer gas planets). Fusion rockets employing planetary refueling at selected locations (e.g., Mars, Callisto, and Titan) could open up the entire solar system to human exploration and colonization.

References

1. Morgan, D.L., "Investigationa of Matter Antimatter Interaction for Possible Propulsion Applications," NASA CR–141356, 1974.
2. Forward, R.L., "Antiproton Annihilation Propulsion," *Journal of Propulsion*, Vol. 1, 1985, p. 370.
3. Forward, R.L., "Exotic Propulsion in the 21st Century," Proceedings of the American Astronautical Society, 33rd Annual Meeting, AAS 86-409, Boulder, CO, Oct. 27–29, 1986.
4. North, D.M., "USAF Focuses Development on Emerging Technologies," *Aviation Week and Space Technology*," Vol. 19, Feb. 24, 1986.
5. Forward, R.L., Cassenti, B.N., and Miller, D. , "Cost Comparisons of Chemical and Antihydrogen Propulsion Systems for High DV Missions," AIAA Paper 85-1455, July 1985.
6. Howe, S.D., Hynes, M.V., Prael, R.E., and Steward, J.D. , "Potential Applicability of the Los Alamos Antiproton Research Program to Advanced Propulsion," Proceedings of the 15th International Symposium on Space Technology and Science, LA-UR-86-1689, Tokyo, Japan, May 19–23, 1986.
7. Forward, R.L., "Antiprotron Annihilation Propulsion," Air Force Rocket Propulsion Lab., AFRPL-TR-85-034, Aug. 15, 1985, p. 55.
8. Altseimer, J.H., et al., "Operating Characteristics and Requirements for the NERVA Flight Engine," AIAA Paper 70-676, June 1970.
9. Ragsdale, R.G., "To Mars in 30 Days by Gas-Core Nuclear Rocket," *Astronautics and Aeronautics*, Vol. 65, Jan. 1972.
10. McNally, J.R., Jr., "Physics of Fusion Fuel Cycles," *Nuclear Technology/Fusion*, Vol. 2, Jan. 1982, p. 9.
11. Wittenberg, L.J., Santarius, J.F., and Kulcinski, G.L., "Lunar Source of He^3 for Commercial Fusion Power," *Fusion Technology*, Vol. 10, Sept. 1986, p. 167.

12. Kulsrud, R.M., Furth, H.P., Valeo, E.J., and Goldhaber, M., "Fusion Reactor Plasmas with Polarized Nuclei," *Physics Review Letters*, Vol. 49, 1982, p. 1248.
13. Adyasevich, B.P., and Fomenko, D.E., "Analysis of Investigation of the Reaction D(d,p)T with Polarized Deuterons," *Soviet Journal of Nuclear Physics*, Vol. 9, 1969, 167.
14. Cassenti, B.N., "Design Consideration for Relativistic Antimatter Rockets," AIAA Paper 81-1531, July 1981.
15. Morgan, D.L., "Concepts for the Design of an Antimatter Annihilation Rocket," *Journal of the British Interplanetary Society*, Vol. 35, 1982, 405.
16. Cassenti, B.N., "Antimatter Propulsion for OTV Applications," AIAA Paper 84-1485, June 1984.
17. Barkas, W.H., and Berger, M.J., "Tables of Energy Losses and Ranges of Heavy Charged Particles," NASA SP-3013, 1964.
18. Peng, Y.-K.M., Strickler, D.J., Borowski, S.K., et al., "Spherical Torus: An Approach to Compact Fusion at Low Field - Initial Ignition Assessments," ANS 6th Top. Mtg. on Tech. of Fusion Energy, San Francisco, CA, March 1985.
19. Katsurai, M., and Yamada, M., "Studies of Conceptual Spheromak Fusion Reactors," *Nuclear Fusion*, Vol. 22, 1982, 1407.
20. Bernabei, S., et al., "Lower-Hybrid Current Drive in the PLT Tokamak," *Physics Review Letters*, Vol. 49, 1982, 1255.
21. Borowski, S.K., "A Physics/Engineering Assessment of a Tokamak-Based Magnetic Fusion Rocket," AIAA Paper 86-1759, June 1986.
22. Stott, P.E., Wilson, C.M. and Gibson, A., *Nuclear Fusion*, Vol. 17, 1977, 481; and *Nuclear Fusion*, Vol. 18, 1978, 475.
23. Yamada, M., "Review of Experimental Spheromak Research and Future Prospects," *Fusion Technology*, Vol. 9, 1986, 38.
24. Dawson, J.M., and Kaw, P.K., "Current Maintenance in Tokamaks by Use of Synchrotron Radiation," *Physics Review Letters*, Vol. 48, 1982, 1730.
25. Bickerton, R.J., Connor, J.W., and Taylor, J.B., "Diffusion Driven Plasma Currents and Bootstrap Tokamak," *Nature, Physics Science*, Vol. 229, 1971, 110.
26. Duderstadt, J.J., and Moses, G.A., *Inertial Confinement Fusion*, Wiley, New York, 1982.
27. Nuckolls, J., Wood, L., Thiessen, A., and Zimmerman, G., "Laser Compression of Matter to Super-High Densities: Thermonuclear (CTR) Application, *Nature*, Vol. 239, 1972, 139.
28. Hyde, R., "A Laser Fusion Rocket for Interplanetary Propulsion," 34th International Astronautical Conf., AIF Paper 83-396, Budapest, Hungary, Oct. 1983.
29. Rom, F.E., "Fast and Moderated Reactors and Applications of Low-Power Nuclear Rockets," *Nuclear, Thermal and Electric Rocket Propulsion*, edited by R.A. Willaume, A. Jaumotte and R.W. Bussard, Gordon and Breach Science, New York, 1967, p. 162.
30. Rom, F.E., "Fast and Moderated Reactors and Applications of Low-Power Nuclear Rockets," *Nuclear, Thermal and Electric Rocket Propulsion*, edited by R.A. Willaume, A. Jaunotte, and R.W. Bussard, Gordon and Breach Science, New York, 1967, p. 75.
31. Ragsdale, R.G. , "Gas-Core Rocket Reactors—A New Look," AIAA Paper 71-641, June 1971.
32. Ragsdale, R.G., "High-Specific-Impulse Gas-Core Reactors," NASA TM X-2243, NASA/Lewis Research Center, March 1971.
33. Rosenbluth, M.N., and Longmire, C.L., *Annals of Physics*, 1957, 1120.
34. Glasstone, S., and Lovberg, R.H., *Controlled Thermonuclear Reactions*, D. Van Nostrand, Princeton, NJ, 1960, p. 336.
35. Rom, F.E., "Nuclear Rocket Propulsion, NASA/Lewis Research Center, TM X-1685, Cleveland, OH, 1968.
36. King, C.R., "Compilation of Thermodynamic Properties, Transport Properties, and Theoretical Rocket Performance of Gaseous Hydrogen," NASA/Lewis Research Center, NASA TN D-275, Cleveland, OH, April 1960.
37. Post, R.F., "Experimental Base of Mirror-Confined Physics," *Fusion*, edited by E. Teller, Academic Press, New York, Vol. 1, Pt. A, 1981, p. 430.
38. Glasstone, S., and Lovberg, R.H., *Controlled Thermonuclear Reactions*, D. Van Nostrand, Princeton, NJ, 1960, p. 31.
39. Glasstone, S., and Lovberg, R.H., *Controlled Thermonuclear Reactions*, D. Van Nostrand, Princeton, NJ, 1960, p. 28.
40. Krall, N.A., and Trivelpiece, A.W. , *Principles of Plasma Physics*, McGraw-New York, 1973, pp. 302–303.
41. Irving, J.H., and Blum, E.K., "Comparative Performance of Ballistic and Low Thrust Vehicles for Flights to Mars," *Vistas in Astronautics*, Vol. 11, Pergamon Press, New York, 1959, p. 191.
42. Shepherd, L.R., "Interstellar Flight," *Journal of the British Interplanetary Society*, Vol. 11, 1952, pp. 149–167.

REPORT DOCUMENTATION PAGE

Form Approved
OMB No. 0704-0188

1. AGENCY USE ONLY (*Leave blank*)	2. REPORT DATE	3. REPORT TYPE AND DATES COVERED
	March 1996	Technical Memorandum

4. TITLE AND SUBTITLE

Comparison of Fusion/Antiproton Propulsion Systems for Interplanetary Travel

5. FUNDING NUMBERS

WU–242–10–01

6. AUTHOR(S)

Stanley K. Borowski

7. PERFORMING ORGANIZATION NAME(S) AND ADDRESS(ES)

National Aeronautics and Space Administration
Lewis Research Center
Cleveland, Ohio 44135–3191

8. PERFORMING ORGANIZATION REPORT NUMBER

E–9712

9. SPONSORING/MONITORING AGENCY NAME(S) AND ADDRESS(ES)

National Aeronautics and Space Administration
Washington, D.C. 20546–0001

10. SPONSORING/MONITORING AGENCY REPORT NUMBER

NASA TM–107030